BULLETIN OF THE CHEMICAL SOCIETY OF JAPAN, VOL. 49 (7), 1766—1771 (1976) [Vol. 49, No. 7

Infrared Absorption Spectrum of Gaseous CF_3CO Radical; Recording on a Rapid-Scan Infrared Spectrometer

Muneteru KOZUKA and Taro ISOBE
Chemical Research Institute of Non-Aqueous Solutions, Tohoku University, Sendai 980

(Received November 27, 1975)

A rapid-scan infrared spectrometer capable of scanning the region from 5000 to 650 cm^{-1} in 200 μs was constructed and successfully applied to study CF_3CO radical produced by flash photolysis. Four absorption bands of the radical were detected at 1574, 1338, 1115, and 1024 cm^{-1} for scanning started 25 μs after the firing of a Xe flash tube. They were tentatively assigned to the CO stretching, CF_3 stretching (a species), CF_3 stretching (e species), and CC stretching vibrations, respectively.

The powerful technique of flash photolysis kinetic (UV-visible) spectroscopy, developed by Norrish and Porter[1)] and Herzberg and Ramsey,[2)] has been extended to the infrared spectral region by Pimentel and his collaborators.[3)] They employed, for the first time, a zinc-doped germanium semiconductor detector[4)] in their rapid-scan infrared spectrometer. The instrument was capable of scanning the region from 5000 to 650 cm^{-1} in several hundred micro-seconds. The scanning speed corresponded to about 100 times the speed of preceding systems developed by other workers.[5)] Using this instrument, they succeeded not only in recording infrared absorption spectra of several new transient intermediates produced by flash photolysis,[3,6—8)] but also in developing the first chemical laser[9)] and the first photodissociation laser.[10)] These new techniques have been successfully used for studying vibrational relaxation processes.[11)]

Therefore, it is now possible to record vibrational spectra of tetratomic or larger transient intermediates, and consequently, to elucidate the mechanisms of many complex reactions. Nevertheless, such studies in the infrared spectral region are very few and many interesting chemical systems remain to be examined, while studies in the UV and visible regions are quite numerous.

The present authors constructed a rather conventional rapid-scan infrared spectrometer and succeeded in detecting CF_3CO radical produced by the flash photolysis of CF_3COI. It is hoped that this instrument will be successively improved by introducing the various new techniques developed in recent years.

Experimental

Materials. NH_3, $COCl_2$, and CO_2 gases were obtained commercially and purified by trap-to-trap distillations. CF_3COI (bp 7 °C) was prepared by a reaction of CF_3COBr (bp 2 °C) with KI. CF_3COBr was obtained by a reaction of CF_3COOH and PBr_3. Immediately before recording the spectra, CF_3COI was decolorized with Cu powder and distilled to eliminate the I_2 released.

Instrument. The instrument consists of a monochromator with a high-speed rotating Littrow mirror, a copper-doped germanium detector (Fujitsu Corp.), a Globar source, a 40-cm quartz gas cell, photolysis flash circuitry and a time base pulse control circuit.

The spectrometer optical path is shown in Fig. 1. In order to protect the detector from the discharge noise of the Xe flash tube, the optical bench of the detector and monochromator sections is separated from that of the Globar source and sample cell sections. This also facilitates the exchange of the light source unit and the sample cell. The collimator mirror, M_8, is an off-axis paraboloidal mirror 60 mm in diameter and with a 280-mm focal length. The rotating Littrow mirror which is made of glass in the form of a tetragonal prism (JASCO Corp.), is used for rapid scanning of the wavelength. Each of the four faces is 50 mm high and 60 mm wide; the face-to-face angles and the face-to-shaft angle are accurate to 6″ and 10″, respectively. The reflecting surfaces are aluminized. The mirror housing is installed on the spectrometer table, while, in order to reduce mechanical vibration, the drive motor (Matsushita Denki Corp., Model SCD-W 150) is set on an independent frame, and both are connected by means of a slender rubber tube (10 mm o.d., 8 mm i.d. and 30 mm long). Rotation at 3000 min^{-1} produces a slight mechanical vibration of the spectrometer table, while rotation at 6000 min^{-1} is well balanced on a frame for adjustment. The mirror scans the 4000—650 cm^{-1} region with a rotation of about 3.3°, so that a speed of 2750 min^{-1} permits the region to be scanned in about 200 μs.

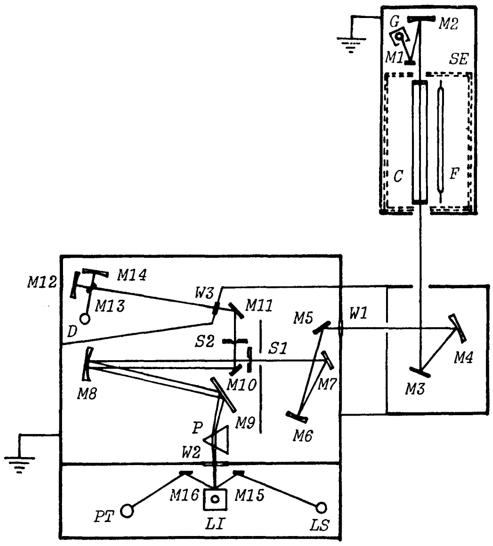

Fig. 1. Optical layout of rapid-scan infrared spectrometer. G: Globar source; SE: electro-magnetic shield; F: Xe flash tube; C: 40 cm quartz gas cell; W_1, W_2, and W_3: NaCl Windows; S_1: entrance slit; S_2: exit slit; P: NaCl prism; M_1, M_3, M_5, M_7, M_{10}, M_{11}, M_{13}, M_{15}, and M_{16}: planar mirrors; M_2, M_4, and M_{12}: spherical mirrors; M_6: troid; M_8: off-axis paraboloid; M_{14}: paraboloid; LI: littrow mirror (tetragonal prism); LS: trigger source (tungsten bulb); PT: phototransistor (OS-14). The light path length from the source to the detector is 4.4 m.

A copper-doped germanium crystal was chosen as the detector on the basis of three criteria: response time, sensitivity, and frequency range. The size is $2.5 \times 5.0 \times 6.0$ mm. One of the faces of area 5.0×6.0 mm is soldered onto a copper cooling holder in specially-designed helium cryostat,[12] using indium and Wood's metal (mp 75 °C). A detector temperature of 4 K was routinely maintained using 1.1 l of liquid helium at reduced pressure (15 mmHg) for 8 h. The temperature was measured with a gold-doped germanium resistor, Cryo Resistor Model CR-1000 (Cryo Cal. Inc.). The background radiation was minimized with a silver film shield maintained at 4 K, an outer copper-plate shield at 77 K, and a KBr plate filter at 77 K. The detector element is visible from the room temperature side through an angle of about 35°. The measured response time was less than 0.05 μs,[13] the detectivity D* (500 K, 1800) 3×10^{10} $cm \cdot Hz^{1/2} \cdot W^{-1}$,[13] the dark resistance 160 kΩ at DC bias current of 50 μA, and the sensitive frequency range approximately 6000—350 cm^{-1}, with maximum sensitivity at about 500 cm^{-1}. The detector leads pass through insulated feed throughs to a small circuit board mounted on the outer wall of the cryostat. This circuit, designed to minimize lead capacitance, contains a power supply (22.5 V dry-cell battery), and a load resistor (100 kΩ carbon-deposited resistor). The signal is fed to a Keithley 102-B wide band preamplifier (2—1.7×10^6 Hz and 0.5—150×10^3 Hz bandpasses available), and then to a synchroscope (Iwasaki Tsushinki Corp., Model SS-5102) equipped with a *Multi-Trace* preamplifier plug-in unit (Iwasaki Tsushinki Corp., Model SP-05M-B). The detector system is shilded with copper and mu-metal screens in order to reduce the discharge noise.

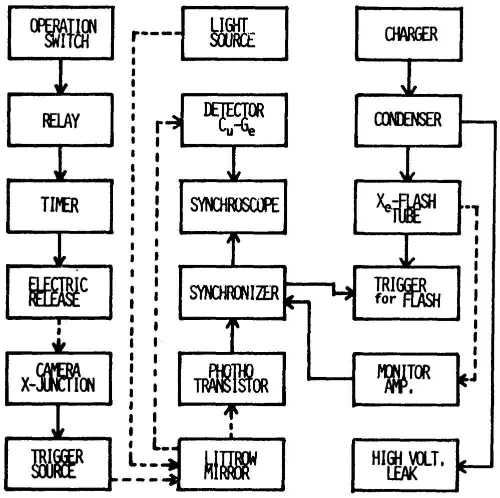

Fig. 2. Block diagram of whole electric system. Real and dotted lines denote electric and optical connections, respectively.

The flash photolysis lamp is a 10 i.d. × 440 mm quartz tube with concentric tungsten electrodes 2 mm in diameter. The lamp is filled with Xe to a pressure of 25 mmHg. The unit is capable of dissipating 600 J in about 20 μs. This energy is supplied by six 8.0 μF condensers charged to 5 kV.

A block diagram of the entire electrical system is shown in Fig. 2. Operation on a micro-second time scale raises special synchronization and recording problem. Firstly, the flash photolysis lamp must be fired, and, after a 25-μs delay for detector recovery, the Littrow mirror must be at the correct angular position to begin the spectral scan. During the next 200 μs, the voltage trace must be recorded. This is accomplished with the specially-designed time-base pulse-control circuit, *Synchronizer*, shown in Fig. 3. When the *Operation Switch* (in Fig. 2) is turned on, the *Electrical Release*, which is made of a speaker magnet coil, pushes the shutter of the camera. The *Trigger Source* bulb connected to the *X-junction* of the camera is lightes. The light beam is reflected by the rotating Littrow mirror and focused onto a silicon phototransistor (OS-14) which produces a pulse each time the mirror passes a given rotational position. The resulting pulse train is amplified, and fed to the *Synchronizer* circuit, where it is used to trigger the synchroscope and the Xe flash tube (point A in Fig. 3). Here, the infrared light and the light for the triggering pulse reflect on the same face of the Littrow mirror for synchronization. The phase relationship between the trigger pulse and the spectral wave length can be adjusted by changing the positions of the phototransistor and the bulb, or alternatively, by changing the delay time in the first delay circuit, DI, in Fig. 3 (point B). In order to obtain stable operation, the first three pulses (point A in Fig. 3) are discarded with the counter circuit, C-2 (point C). The fourth pulse releases the HOLD circuit from clamping (point D) and the fifth passes through the first switching circuit, SWI, to the second delay circuit, DII (point E). The voltage drop in one of the DII collectors (point G') forces the third delay circuit, DIII, to generate a delayed pulse (point F), and the voltage rise of the pulse, in turn, induces a 2 μF condenser (in *Trigger for Flash* circuit in Fig. 2) to discharge through a thyratron (Toshiba Corp., 1G50A). A fly-back transformer (Chuo Musen Corp., TV-304 CD 3) connected to the thyratron generates a trigger pulse of about 20 kV which fires the charged Xe flash tube. A portion of the flash light is fed to a photomultiplier (Hamamatsu Televi Corp., R-252) in the *Monitor Amp.* circuit in Fig. 2. The resultant signal is amplified and used to release the second switching circuit, SW-II, from clamping (point H and I in Fig. 3). Finally, the output signal of the DII (point G) arrives at the synchroscope either *via* a counter circuit, C-8, or directly (point J). The C-8 is used to thin out some pulses in the train for the purpose of recording the spectra of fairly long-lived intermediates (life time: 0.1—1.0 s). By adjusting the delay times of DII and DIII, one can set the sweep of the synchroscope to the moment desired after the flash terminates.

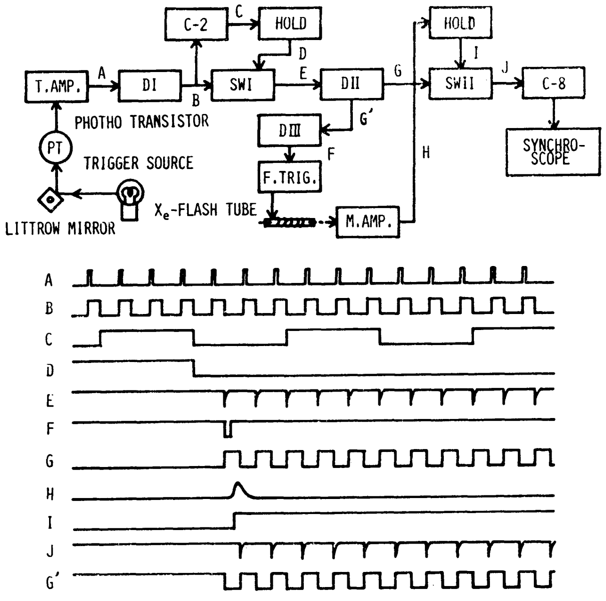

Fig. 3. Block diagram of time base pulse control system (synchronizer) and its timing chart. T. Amp.: amplifier for trigger pulse, F. Trig.: trigger for flash, M. Amp.: monitor amplifier.

Results and Discussion

Instrument Performance. Reference spectra of air, $COCl_2$ and NH_3 were recorded on the instrument equipped with an NaCl prism and a Globar source. Immediately before every run, the light source was adjusted to a white glow (1300—1600 °C), and the Littrow mirror was set to high-speed rotation (about 3000 min^{-1}). Dried N_2 gas was blown through the light path, as necessary.

The 1.7 MHz amplifier bandpass increases the noise level by a factor of 1000 over that of narrow bandpass amplifiers normally used in thermocouple spectrometers. Therefore, reducing this noise is essential to rapid-scan infrared spectroscopy. To facilitate the estimation of the absolute value of this noise in various recording conditions, the narrowest possible slit width and the highest possible gain of the detector system were used throughout the experiment. Because of the resultant low S/N, it became very difficult to quantitatively control the influence of the following factors which dominate the spectral resolution, the band shape and the band intensity: the brightness of the light source, the rotating speed of the Littrow mirror, the selection of the wavelength region, the gain of the detector system, the sweep speed of the synchroscope, *etc.* The S/N may be estimated from the ratio of the intensity to the thickness of the voltage trace. Throughout the experiment, it was 38—43 at 3000 cm^{-1} and 4—8 at 1000 cm^{-1}.

The thickness of the voltage trace was investigated using a *wave analyser* (General Radio Company Concord, USA, Type 1900-A). It was found that the thickness was due to white noise of about 100 μV and not due to any hum. The noise increased exponentially below 100 Hz. This agrees well with the noise characteristics of a CuGe detector. The Keithley 102-B preamplifier has a noise level of 20 μV in case of short-input circuit, a gain of 60 dB and a 1.7 MHz bandpass. The noise signal appears as high as 50—60 μV on the synchroscope. This would build up the 100 μV white noise along with the noise contributions due to the CuGe detector and load resistor. Besides this high frequency noise, there was a microphonic noise of 50—100 μV and of about 100 Hz, which is caused by the mechanical vibration accompaning the rotation of the Littrow mirror.

Although the time constant of the entire detector system could not be measured precisely because of the microphonic noise, it was observed that the intensity of the voltage trace at a scanning speed of 1000 min^{-1} did not decrease at speeds up to 3000 min^{-1}.

Figure 4 shows the atmospheric absorption spectrum due to ν_{OH} (3654)* and δ_{OH} (1595) of H_2O, and due to ν_{CO} (2349) of CO_2. Each of the four voltage traces corresponds to scanning by each of the four faces of the Littrow mirror. Under the conditions, it may be said that the spectral resolution is independent of the face. The microphonic noise slightly shifts the starting point of the first (lowest) sweep in Fig. 4 with respect to the starting points of the other sweeps. Wave number calibration was carried out on the basis of the absorption bands for which vertical short lines were drawn. Because the reflecting faces of the Littrow mirror are separated from the rotating axis by 25 mm, the nonlinearity in the wave number scale is emphasized, as compared with that in the case of a planar Littrow mirror. Figure 5 shows the absorption bands due to $COCl_2$. In addition to the two fundamental frequencies,

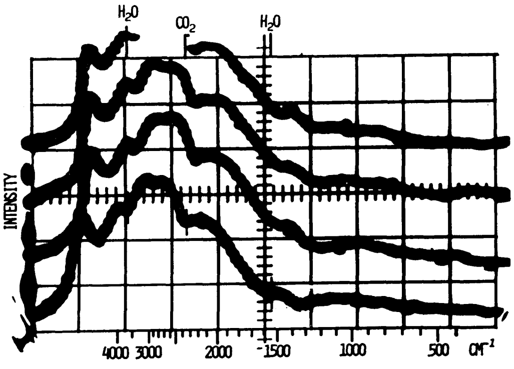

Fig. 4. Atmospheric absorptions. 150 μ slits, sweep 20 μs/div., 0.5 mV/div. The evacuated 40 cm qrtz gas cell was set in the light path.

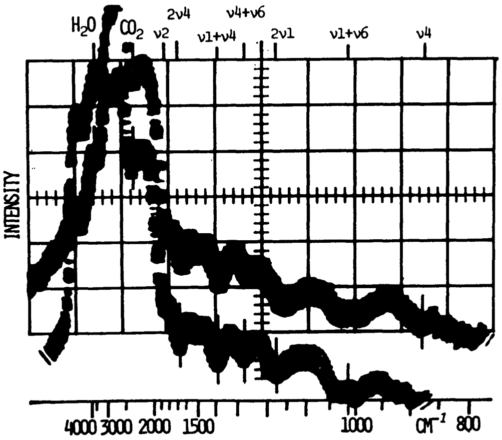

Fig. 5. Absorptions due to $COCl_2$ and atmosphere. 150 μ slits, sweep 50 μs/div., 0.2 mV/div., 40 cm gas cell, 30 mmHg $COCl_2$.

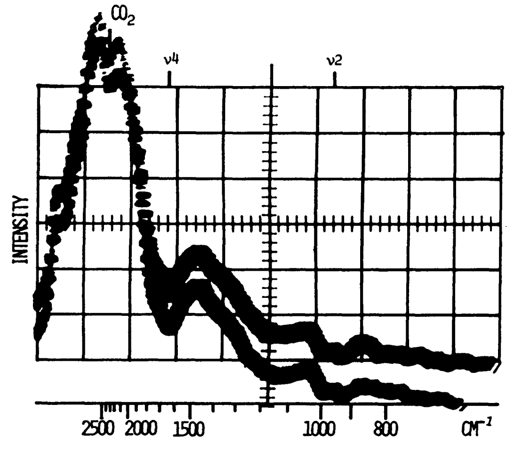

Fig. 6. Absorptions due to NH_3 and atmosphere. 300 μ slits, sweep 50 μs/div., 0.3 mV/div., 40 cm gas cell, 30 mmHg NH_3.

---

* Numerals in parentheses denote the wave numbers of the absorption bands.

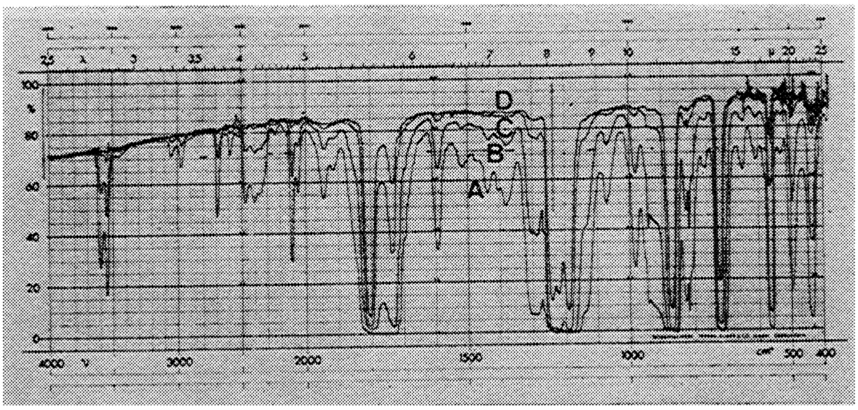

Fig. 7. Infrared spectrum of CF_3COI recorded on a Perkin-Elmer Model 125 Spectrometer with use of 10 cm gas cell: (A) 25 mmHg, (B) 15 mmHg, (C) 8 mmHg, (D) 3 mmHg.

ν_2 (1827) and ν_4 (849), five combination bands, $2\nu_4$ (1677), $\nu_1+\nu_4$ (1412), $\nu_4+\nu_6$ (1276), $2\nu_1$ (1159) and $\nu_1+\nu_6$ (1011), are recorded. Figure 6 shows the HNH deformation mode, ν_4 (1627.5), and the umbrella mode, ν_2 (931.58 and 968.08), of NH_3.[14]

From these spectra, it is seen that the instrument is quite adequate for qualitative low-resolution detection of transient intermediates with half-lives as short as 50 μs.

Application. CF_3COI was chosen as the first chemical system for exploration on the basis of the following criteria: (1) high infrared absorption coefficients of the CF and CO stretching vibrations, (2) a high photolytic yield for the breaking of the CI bond, (3) its chemical interest, and (4) an adequate vapor pressure at room temperature. Prior to the experiment, INDO calculations were carried out to estimate the minimum CC-bond distances for CF_3COF, CF_3COH, CF_3CN, and CF_3CO radicals, since sufficient information about these molecular parameters could not be obtained in other ways. The following assumptions were made: CF (in CF_3) 1.34 Å, CO 1.19 Å, CH 1.09 Å,[15] CN 1.15 Å, $\angle$FCF (in CF_3) 109°28′,[15] and $\angle$HCO 120°.[15] The calculated values were 1.50, 1.49, 1.47, and 1.42 Å, respectively. These values suggest that the CC stretching vibration in the CF_3CO radical couples strongly with the CF and CO stretching vibrations, and consequently the fundamental frequencies of the radical are fairly different from those of CF_3COI.

Since no IR spectrum of CF_3COI has yet been published, the one recorded on the Perkin-Elmer 125 spectrometer is shown in Fig. 7. Absorption bands at 1806, 1240, 1190, and 870 cm^{-1} were approximately assigned to ν_{CO}, ν_{CF_3}, ν_{FCF_2}(a'), ν_{FCF_2}(a''), and ν_{CC}, respectively. When the sample pressure is high, the absorption maxima are shifted from the fundamental frequencies. This was taken into account in the wave number calibration in Fig. 8. Spectra (A), (B) and (C) in Fig. 8 were recorded on the instrument before, immediately after, and about two seconds after photolysis, respectively. ν_{CO} of CO_2 was recorded in (A), besides ν_{CO}, ν_{CF}'s, and ν_{CC} of CF_3COI. The first and the second traces are slightly shifted with respect to each other. This could also be because of microphonic noise as in the case of Fig. 4. In (B), dried N_2 gas was

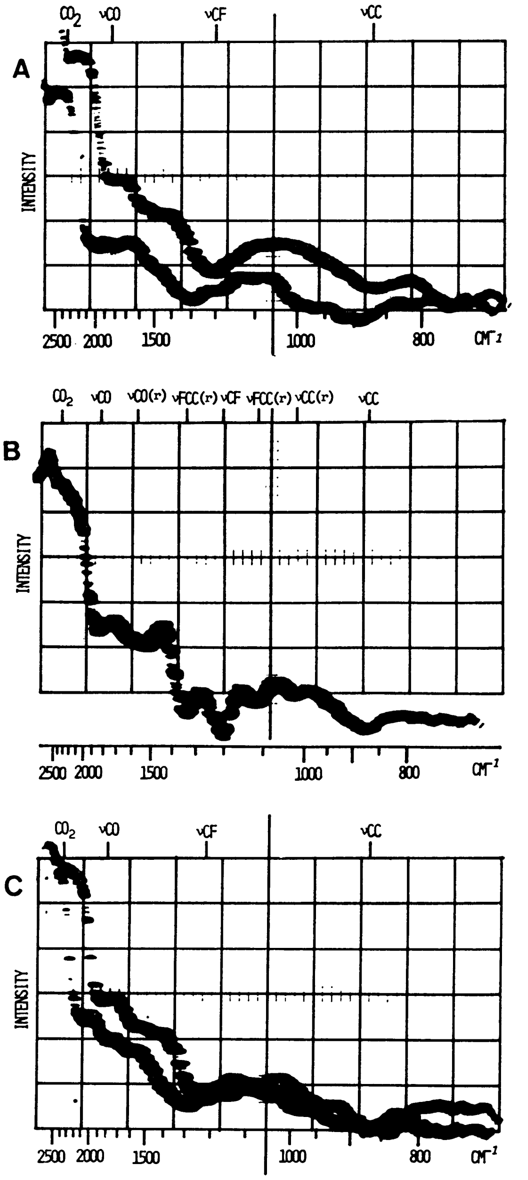

Fig. 8. Flash photolysis of CF_3COI: 200 μ slits, sweep 20 μs/div., 0.2 mV/div., 40 cm gas cell, 40 mmHg CF_3COI, N_2 700 mmHg, (A) Before Photolysis, (B) Immediately after photolysis, (r) denote radical, (C) About 2 s after photolysis.

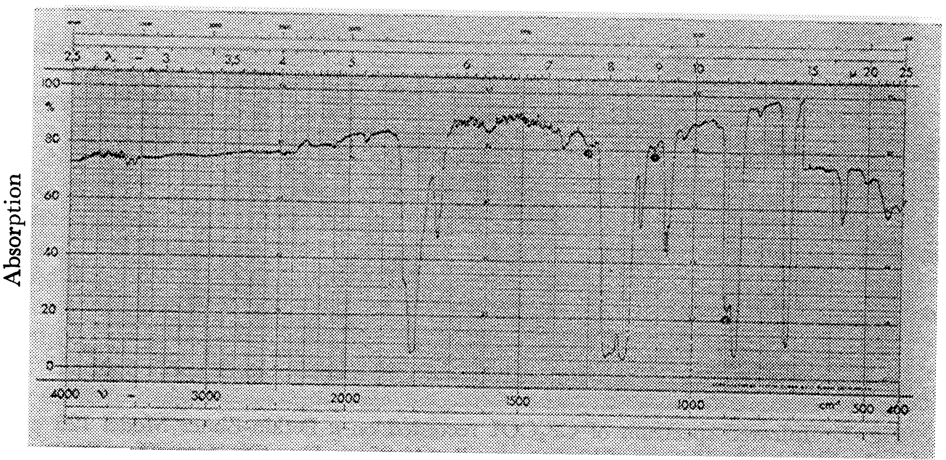

Fig. 9. Infrared spectrum of decomposition products in CF_3COI flash-photolysis: * denote absorption due to C_2F_5I.

blown through the optical path. Spectrum (B) was swept 25 μs after trigger pulse was fed to the charged Xe flash tube. Although the *Multi Trace* unit was set to sweep twice, only one voltage trace was recorded. This could be caused by tailing of the flash noise. Prior to this experiment, it was ascertained that any single sweep, for which the *Multi Trace* unit acts only as an ordinary preamplifier, was performed normally and consistently at 25 μs after photolysis, but not at 13 μs. Therefore, the trace in (B) is undoubtedly the first sweep, but not the second (about 5 ms later). In addition to the absorption bands due to CO_2 and CF_3-COI, four new absorption bands were detected at 1574, 1338, 1115 and 1024 cm^{-1}. They did not appear in (C). Their absolute intensities were difficult to estimate because of the microphonic noise, but the sensitivity of this instrument in the relevant spectral region is confirmed in Figs. 5 and 6. The CF_3CO radical population should be smaller than the $COCl_2$ and NH_3 populations, while the absorption coefficient of the radical should be larger than those of the combination bands and of the umbrella mode in the molecules. Therefore, it is thought that the data are quite adequate for qualitative discussion. The decomposition products were transfered into a 10 cm gas cell, and the infrared spectrum was recorded on a Perkin-Elmer 125 spectrometer (Fig. 9). The CF_3COI pressure decreased to one tenth of the value before photolysis. The absorption in the 1800 cm^{-1} region suggests that there is no perfluorobiacetyl, $(CF_3CO)_2$. The absorption bands at 1321, 1113, and 923 cm^{-1} should be due to C_2F_5I. In addition, there are uncondensed molecular species at liquid N_2 temperature. They are CO (2100), C_2F_6 (1113), CF_4, CF_3I, *etc.* The light intensity of the Xe flash tube has the peak in the wavelength region of 300—400 nm. The CI bond is usually ruptured by the light, but the CF, CC and CO bonds are not. All of these suggest that the photolysis produces, first, a CF_3CO radical in the electronic ground state, and then the radical decomposes into a CF_3 radical and CO, either due to room light or thermal collisions. This explanation is in good agreement with the results of Noda *et al.*[16] that the CH_3CO radical in an isolated matrix at liq. N_2 temperature is easily decomposed by visible light into a CH_3 radical and CO.

Consequently, it is concluded that the four weak and transient absorptions in Fig. 8 (B) are due to the CF_3CO radical. They were tentatively assigned to ν_{CO} (1574), ν_{CF_3} (1338, a species), ν_{CF_3} (1115, e species), and ν_{CC} (1024). They should be coupled strongly to each other.

The authors wish to thank the Ministry of Education for financial support for this study. They also wish to express their gratitude to the (late) Prof. Kozo Kamiryo, Dr. Katsuhiko Ishida, Messrs. Kiichi Sato and Setsuo Tamagawa of the Research Institute of Electrical Communication of this university, and to Messrs. Minoru Takahashi and Eijiro Yamazaki of this institute, who assigned in the construction of the liquid He cryostat. The authors also gratefully acknowledge Prof. Tsuneo Ikenoue and his collaborators of this institute for assistance in constructing the electric circuits, and the (late) Professors Susumu Kinumaki and Tetsuo Hata, Mr. Shinji Onodera and Mrs. Hamako Sato of this institute for their assistance in earlier stages of this work.

References

1) R. G. N. Norrish and G. Porter, *Nature*, **164**, 658 (1949).

2) G. Herzberg and D. A. Ramsey, *Discuss. Faraday Soc.*, **9**, 80 (1950).

3) G. C. Pimentel and K. C. Herr, *J. Chim. Phys.*, **1964**, 1509; K. C. Herr and G. C. Pimental, *Appl. Opt.*, **4**, 25 (1965).

4) M. E. Lasser, P. Cholet, and E. C. Wurst, *J. Opt. Soc. Am.*, **48**, 468 (1958); H. Levinstein, *Proc. Inst. Radio Engnrs.*, **47**, 1478 (1959); L. Johnson and H. Levinstein, *Phys. Rev.*, **117**, 1191 (1960).

5) B. W. Bullock and S. Silverman, *J. Opt. Soc. Am.*, **40**, 608 (1950); E. F. Daly, *Nature*, **166**, 1027 (1950); P. W. Wheatly, E. R. Vincent, D. L. Rotenberg, and G. R. Cowan, *J. Opt. Soc. Am.*, **41**, 665 (1951); D. A. H. Brown and V. Roberts, *J. Sci. Instr.*, **30**, 5 (1953).

6) R. J. Jensen and G. C. Pimentel, *J. Phys. Chem.*, **71**, 1803 (1967).

7) G. A. Carlson and G. C. Pimentel, *J. Chem. Phys.*, **44**, 4035 (1966).

8) L. Y. Tan, A. M. Winer, and G. C. Pimentel, *J. Chem. Phys.*, **57**, 4028 (1972).

9) J. V. V. Kasper and G. C. Pimentel, *Phys. Rev.*, **14**, 352 (1965).

10) J. V. V. Kasper and G. C. Pimentel, *Appl. Phys. Lett.*, **5**, 231 (1964).

11) R. D. Coombe and G. C. Pimentel, *J. Chem. Phys.*, **59**, 251 (1973).

12) Details will be reported elsewhere.

13) T. Yamaoka and Y. Ueda (Fujitsu Corp.), private communication.

14) H. Y. Sheng, E. F. Barker, and D. M. Dennison, *Phys. Rev.*, **60**, 786 (1941); *Sadtler* 95B.

15) R. H. Schwendeman, *Diss. Abs.*, **18**, 1645 (1958).

16) S. Noda, K. Fueki, and Z. Kuri, *J. Chem. Phys.*, **49**, 3287 (1968).